MTI focal plane assembly design and performance

Jeffrey L. Rienstra*[a], Mary Ballard[b]

[a]Sandia National Laboratories, P.O. Box 5800, MS 0972, Albuquerque, NM 87185-0972

[b]Raytheon Infrared Center of Excellence, 75 Coromar Dr., Bldg B3, M/S 92, Goleta, CA 93117

ABSTRACT

The focal plane assembly for the Multispectral Thermal Imager (MTI) consists of sensor chip assemblies, optical filters, and a vacuum enclosure. Sensor chip assemblies, composed of linear detector arrays and readout integrated circuits, provide spatial resolution in the cross-track direction for the pushbroom imager. Optical filters define 15 spectral bands in a range from 0.45 μm to 10.7 μm. All the detector arrays are mounted on a single focal plane and are designed to operate at 75 K. Three pairs of sensor chip assemblies (SCAs) are required to provide cross-track coverage in all 15 spectral bands. Each pair of SCAs includes detector arrays made from silicon, indium antimonide, and mercury cadmium telluride. Readout integrated circuits multiplex the signals from the detectors to 18 separate video channels. Optical filter assemblies defining the spectral bands are mounted over the linear detector arrays. Each filter assembly consists of several filter strips bonded together side-by-side. The MTI focal plane assembly has been integrated with the rest of the payload and has undergone detailed testing and calibration. This paper includes representative test data for the various spectral bands and the overall performance of the focal plane assembly.

Keywords: Multispectral imaging, focal plane arrays, remote sensing

1. INTRODUCTION

The purpose of this paper is to describe the focal plane assembly for the Multispectral Thermal Imager satellite. Multispectral remote sensing from space has been provided for quite some time by a number of existing systems. Examples are Landsat Thematic Mapper (TM)[1], Advanced Very High Resolution Radiometer (AVHRR)[2], and SPOT (Satellite Pour l'Observation de la Terra)[3]. These multispectral imaging systems provide a wealth of useful information relating to earth resources and environmental monitoring. TM and AVHRR cover the range of wavelengths from the visible to long wavelength infrared but use scanning optics to form an image and beam splitters to divide the spectral content onto several focal planes. SPOT is a pushbroom imager with long, linear arrays, but it only covers visible to near infrared wavelengths and also uses beam splitters with several focal planes. In this paper we describe an advanced focal plane assembly that embodies a unique, straightforward, and simple design for multispectral imaging over a broad range of wavelengths. The MTI approach is based on a single focal plane with 15 spectral bands in a pushbroom imager.

The next section of this paper is a general description of the overall sensor system and short description of the subsystems. Section three contains a more detailed description of the focal plane assembly (FPA) and its major components, including the detector arrays, readout integrated circuits, and optical filters. The following section identifies the most significant FPA performance parameters and a summary of the test data obtained at the FPA level. The last section is a summary.

2. SENSOR DESCRIPTION

2.1. General

The objective of building this research and development multispectral sensor is to demonstrate and evaluate advanced multispectral imaging technologies for satellite remote sensing.[4] The imaging system consists of the telescope, focal plane, cryogenic cooler, and sensor electronics, making up a multispectral, pushbroom type imaging system.[5] Linear detector arrays with optical filters immediately above the arrays are placed at the focal plane of the telescope. The linear arrays provide spatial resolution in one direction (cross-track). The motion of the satellite relative to the ground produces a scanning operation in the other direction (along-track), thereby producing two-dimensional images in multiple wavelength bands. The multispectral images are stored in on-board memory and then sent to the ground for archiving and processing.

* Correspondence: Email: jlriens@sandia.gov; Telephone: 505-845-8682; Fax: 505-844-0906

DISCLAIMER

Table 1 shows the designations for the 15 MTI bands. All the bands lie between 0.45 μm and 10.7 μm. The first four are usually referred to as the visible (VIS) bands. The next three bands are the near infrared (NIR). Following that are three short wavelength infrared (SWIR) bands and two medium wavelength infrared (MWIR) bands. The last three bands are the long wavelength infrared (LWIR) bands. Individual bands are referred to by letter, A through O. Band O was added after the other bands were identified, which explains why it is out of sequence.

Table 1. Sensor spectral bands.

Band	Wavelength range (μm)	Characteristics
A	0.45 - 0.52	VIS (blue)
B	0.52 - 0.60	VIS (green)
C	0.62 - 0.68	VIS (red)
D	0.76 - 0.86	VIS (deep red)
E	0.86 - 0.89	NIR
F	0.91 - 0.97	NIR
G	0.99 - 1.04	NIR
H	1.36-1.39	SWIR
I	1.55 - 1.75	SWIR
O	2.08 - 2.35	SWIR
J	3.50 - 4.10	MWIR
K	4.87 - 5.07	MWIR
L	8.00 - 8.40	LWIR
M	8.40 - 8.85	LWIR
N	10.2 - 10.7	LWIR

The MTI sensor incorporates a single focal plane design; no beam splitters are used. This is in contrast with the other sensor systems mentioned above. All of them use beam splitters and more than one physical focal plane to include all the spectral bands. All detectors in the MTI sensor system are maintained at the same temperature, nominally 75 K, with a long-life cryogenic cooler.

One of the overriding considerations in the design of this sensor system is radiometric accuracy. The MTI payload has undergone extensive laboratory calibration. In addition, a built-in calibration system will be used to monitor performance of the imaging system and to correct for drift in detector output.

2.2. Telescope

The MTI telescope is a three-mirror anastigmat design.[6] The unobscured telescope design provides aperture diffraction limited performance in the LWIR bands and very respectable performance in the shorter wavelength bands as well. The mirrors are uncooled, and the telescope cavity is maintained at approximately 275 K. The telescope design provides an exit pupil which is accessible and allows very effective cold shielding of the warm optical structure.

2.3. On-Board Calibration System

The telescope includes several subassemblies that make up the on-board calibration system. The aperture door is double hinged to allow two different surfaces to fill the telescope field of view to provide end-to-end calibration of the imaging system. In the door closed position, the aperture door assembly constitutes a temperature-controlled blackbody radiator for calibrating the MWIR and LWIR detector channels. In the door open position, a diffuse reflective panel can be opened up to allow reflected sunlight to illuminate the VIS, NIR, and SWIR detectors. In addition, there is a quick calibration wheel inside the telescope near the FPA. An incandescent lamp and two blackbody sources at different temperatures can be placed in view of the detectors within seconds of an imaging sequence to mitigate the effects of detector drift. One of the wheel positions is a retroreflector to provide a low level infrared signal and to reduce the radiative heat load from the warm telescope cavity onto the focal plane assembly.

2.4. Cryocooler

The cryocooler provides over 3 watts of cooling power at 65 K. A thermal strap connects the cold block of the cryocooler to the pedestal that supports the detector arrays. The cryocooler also cools the cold shield to reduce the infrared background on the focal plane. The cryocooler uses temperature sensors to provide closed loop temperature control of the cold block. It is designed for low vibration to minimize jitter of the imaging system.

2.5. Sensor Electronics

The sensor electronics subsystem performs a number of functions related to the focal plane assembly, the telescope, and the cryocooler. The electronics subsystem provides timing and control signals to the focal plane readout circuits as well as high resolution temperature control of the focal plane. The functions relative to focal plane image data include amplification and digitization of serial data from the focal plane readout circuits, image compression, data storage, and data encoding.

3. FPA DESCRIPTION

3.1. General Description

3.1.1. Mechanical Configuration

Figure 1(a) shows a cutaway view of the focal plane assembly which illustrates the mechanical configuration of the unit. The three SCA pairs are mounted on individual motherboards which have electrical traces to conduct control waveforms and analog signals between the SCAs and the cables. The cryogenic cables complete the connection between the cold focal plane and the cable connectors attached to the warm part of the assembly. A filter assembly positions the cold optical filters directly above the appropriate detector arrays. The cold shield minimizes the infrared background on the detector arrays and maintains a stable operating environment. Finally, the vacuum enclosure surrounds the focal plane components and allows the SCAs and filters to be cooled during laboratory testing. Figure 1(b) is a photograph of the fully assembled flight unit.

One of the principal challenges of this design is to maintain the relative height of the individual SCAs within very tight tolerances. The extremely short depth of focus of the telescope demands that the height variation be less than ±15 μm for the VIS bands, ±30 μm for the NIR - MWIR bands, and ±50 μm for the LWIR bands.

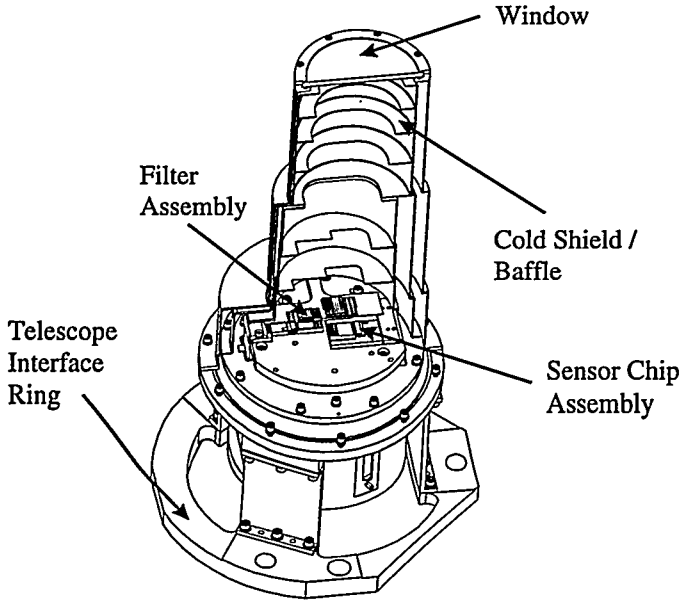

Figure 1(a). Cutaway view of focal plane assembly.

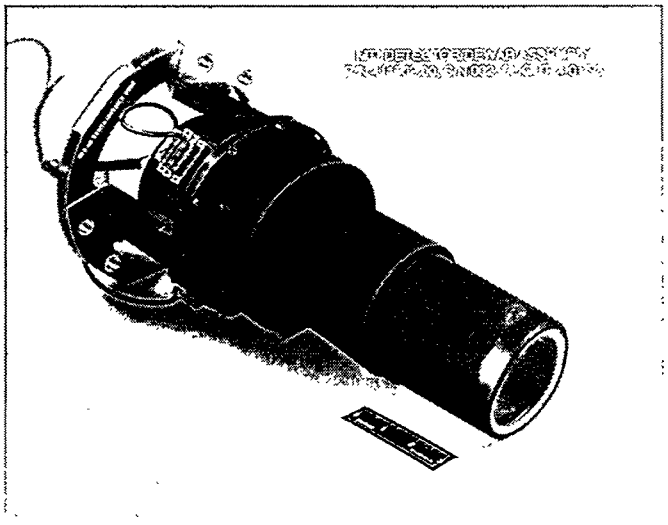

Figure 1(b). MTI focal plane assembly.

A thermal-mechanical mockup of the focal plane assembly was fabricated for qualification level vibration tests and to check out mechanical interfaces. Thermal tests were also performed to measure the thermal load presented by the unit to the cryocooler. This mockup did not include sensor chip assemblies but did include resistors that were used to simulate electrical power dissipation of the SCAs. The thermal-mechanical mockup was then partially populated with engineering grade SCAs to test electrical and optical interfaces before the flight FPA was delivered.

3.1.2. Focal Plane

The cross-track dimension of the MTI focal plane is nearly 30 mm. It would be extremely difficult with today's technology to build MWIR or LWIR detector arrays to cover the entire cross-track dimension with a single linear array. Therefore, three staggered linear arrays are used for each spectral band. The visible wavelength through mid-wavelength infrared bands are grouped on one sensor chip assembly (SCA), and the long wavelength infrared bands are grouped on a different SCA. One VIS/MWIR SCA is paired with one LWIR SCA to cover approximately one third of the cross-track dimension; three staggered SCA pairs are used to span the full cross-track field of view. The arrangement of the SCAs on the focal plane is shown in Figure 2(a). A photograph of the SCAs on the focal plane pedestal is shown in Figure 2(b).

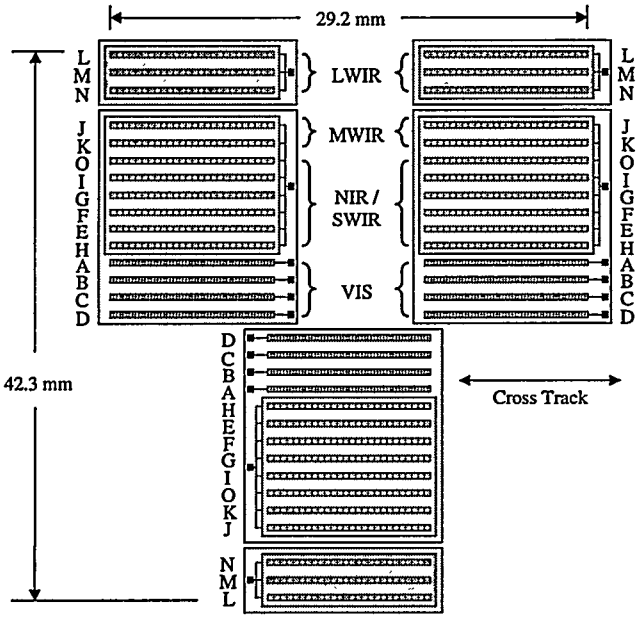

Figure 2(a). Focal plane layout.

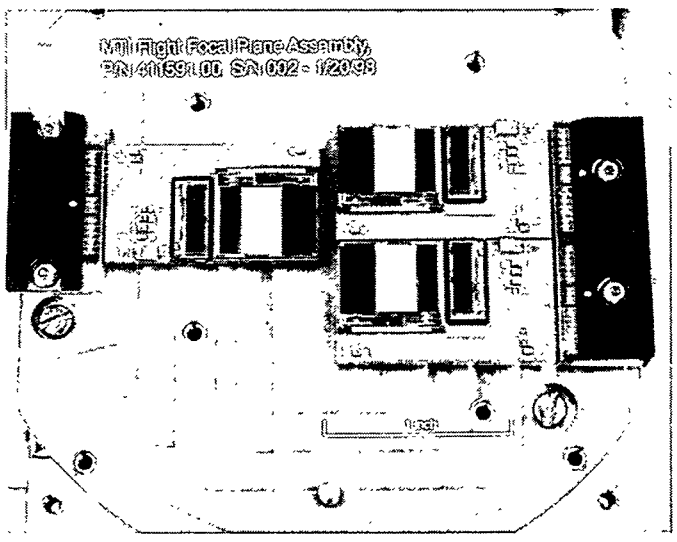

Figure 2(b). SCAs on focal plane.

Three different detector materials are used for the various wavelengths. Silicon photodiodes are used for bands A-D. Indium antimonide is used for bands E-K and O. Mercury cadmium telluride is used for bands L-N. The order of the bands on the focal plane is also shown in Figure 1. The particular order of bands was chosen to keep the detector arrays made of the same material grouped together and to meet image quality requirements.

With the exception of band A-D these SCAs use hybrid focal plane array technology[7,8], wherein an array of backside-illuminated photodetectors is attached with cold-welded indium interconnects to a readout integrated circuit (ROIC). The ROIC has a capacitive-feedback transimpedance amplifier corresponding to each pixel which amplifies and stores the signal from the detector. Multiplexing circuitry on the ROIC produces a serial output of values which can be digitized, stored, and processed.

3.2. FPA Components

3.2.1. Detector Arrays

The front side illuminated detector arrays for bands A-D are formed in the same silicon chip that makes up the ROIC for the InSb detectors. There are 828 photodiode detectors per SCA for each of the four visible bands. Photodiodes were chosen to ensure high performance at the operating temperature of 75 K. The pixels are 12.4 μm square and are laid out in two staggered rows separated by 12.4 μm. The layout of the silicon photodiode detectors is shown in Figure 3(a). A guard ring surrounds each individual pixel, reducing the cross-talk between pixels and enhancing spatial resolution. The active detector area for each pixel is defined by an aperture in the opaque coating that is applied to the silicon surface. This opaque coating shields the amplifiers and multiplexing circuitry from incident light.

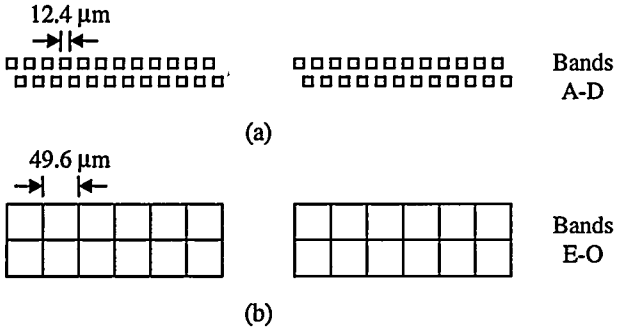

Figure 3. Detector array layout.

Bands E-K and O utilize InSb photodiode detectors. These back side illuminated detectors are fabricated within a single piece of InSb which is hybridized to a silicon chip containing the readout circuitry for these bands as well as the detectors and readouts for bands A-D. There are 207 detectors per SCA for each of the bands E-K and O. The pixels for these bands are 49.6 μm square. The layout of the InSb detectors is shown in Figure 3(b). Two rows of detectors are fabricated for each of the InSb bands. This provides a primary and an alternate pixel, individually selectable. For all the InSb bands except H, pixel selection circuitry in the ROIC is used to connect either the primary or the alternate detector to the readout, thereby achieving near 100% pixel operability. Both rows of band H detectors are read out so they can be combined later to improve the signal-to-noise ratio.

The detector arrays for bands L-N are made from HgCdTe. These bands also have 207 pixels per SCA, with 49.6 μm square pixels. Like the InSb detectors, two rows of photodiodes are made for each band and pixel selection is used to increase operability. These bands utilize a separate ROIC chip from the other bands to increase overall SCA yield.

3.2.2. Readout Integrated Circuits

The ROICs for all the bands are based on a common amplifier design for the unit cells. A capacitive-feedback transimpedance amplifier (CTIA)[9] is used to integrate photocurrent from the corresponding detector and convert the electrical charge into a voltage which can be multiplexed with the signals from other detectors and read out. This circuit design provides very low noise and good linearity over a broad range of irradiance conditions.

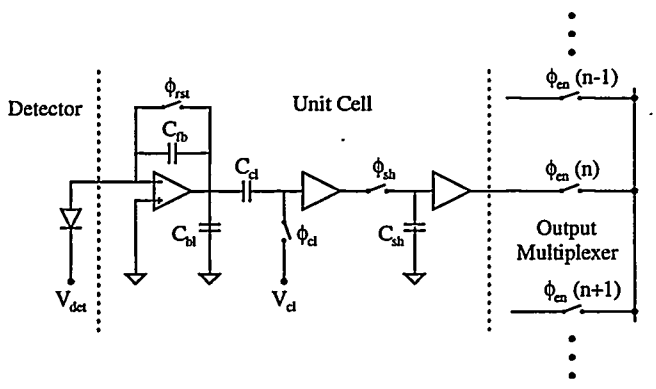

Figure 4. Unit cell schematic.

A simplified schematic of the unit cell amplifier is shown in Figure 4. This shows the CTIA which integrates photocurrent during each frame. The switch controlled by the clock, ϕ_{rst}, resets the integrator. A band limiting capacitor reduces the noise bandwidth of the amplifier. The switch controlled by ϕ_{cl} works in conjunction with ϕ_{rst} to level shift the signal and to reduce the reset noise of the feedback capacitor by a technique called correlated double sampling. Following a buffer amplifier, the signal is transferred to the sample and hold capacitor by ϕ_{sh}. This allows all the pixels to be sampled and reset simultaneously and the signal corresponding to each pixel to be read out sequentially during the next integration period. A second

buffer amplifier is used for driving the signal out of each unit cell onto the signal bus when it is accessed by ϕ_{en}. Not shown is the output amplifier on the video line which drives the serial data stream off chip.

The total data rate from the focal plane is determined by the number of pixels and the frame time. The nominal frame time for bands A-D and L-N is 715 μs, and the nominal frame time the other bands is 2.86 ms. There are a total of 2,484 pixels in each of bands A-D and 621 pixels in each of the other bands. Including the fact that both the primary and alternate pixels for band H are read out, the total data rate for the focal plane is approximately 18.5 megapixels per second.

Even though a common circuit design is used for all the spectral bands, some tailoring is required to accommodate different background signal levels expected for each band and to meet different sensitivity requirements. These differing requirements can be fulfilled for the most part by changing the value of the feedback capacitor in the unit cell. A larger capacitor allows for exposure to higher irradiance levels without saturating. A smaller capacitor provides a larger conversion gain from photocurrent to output voltage.

One of the features of the ROIC design is a variable integration time. The clock waveforms that activate the reset, clamp, and sample switches determine what fraction of the total frame time is used for integrating photocurrent and leakage current. This value can be changed during operation of the sensor in accordance with operating experience and the expected irradiance levels for a particular imaging sequence. Variable integration time essentially becomes a variable gain setting which can be used to make the most of the available dynamic range of the ROIC.

3.2.3. Filter Assembly

The function of the filter assembly is to position optical filters over the detector arrays to define the appropriate spectral bands. The filters are attached to the focal plane and operate at nearly the same temperature as the focal plane to reduce the infrared background.

The filters must be mechanically fixed above the detector arrays. Groups of filters are bonded together, side-by-side into filter assemblies. The VIS-MWIR bands make up one group and the LWIR bands are the other. These filter assemblies are bonded to a metal bezel which is attached to the focal plane pedestal. Figure 5(a) shows the arrangement by representing a cross-section of the focal plane in the along-track direction. Figure 5(b) is a photograph of the filter assemblies mounted in the filter bezel and installed over the SCAs on the focal plane pedestal.

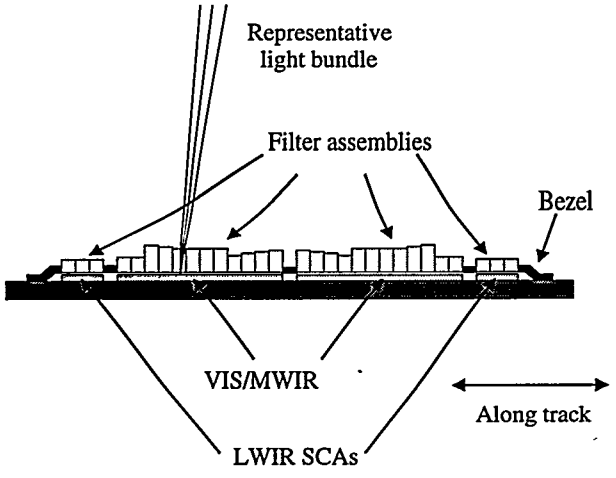

Figure 5(a). Edge view of filter/bezel assembly.

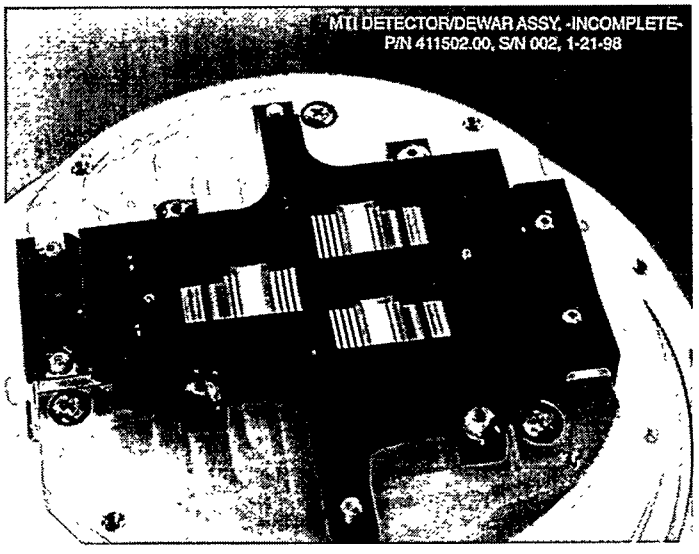

Figure 5(b). Filter assemblies with bezel.

The optical filters must pass the desired range of wavelengths and reflect or absorb wavelengths outside that range. To maintain radiometric accuracy the out-of-band blocking must be extremely effective. The filters use multilayer dielectric films to define the pass bands. Other layers are added to form low-pass or high-pass blocking layers. A composite filter substrate, including a layer of absorbing glass, is used for some bands.

The thickness of each filter is tailored to equalize the focus for each spectral band. Due to the different materials used for the filter substrates and the change in index of refraction with wavelength, the total focus shift introduced by these materials is different. The thickness of each filter substrate is calculated so that the focus for each band will occur at the appropriate place.

3.2.4. Motherboard/Cryogenic Cables

A separate motherboard is used for each SCA pair. One VIS/MWIR SCA and one LWIR SCA are attached to a motherboard which in turn is attached to the focal plane pedestal. Wire bonds are used to connect the SCAs to electrical traces on the motherboard. At the edge of the pedestal are cryogenic cables which are wirebonded to the motherboard traces and carry the electrical signals from the cold focal plane region to the relatively warm vacuum enclosure. These cables must have good electrical conductivity but low thermal conductivity to minimize the thermal load of the focal plane assembly on the cryocooler.

3.2.5. Cold Shield

The cold shield performs two major functions. The first is to limit the field of view of the warm telescope structure from the focal plane, reducing the background irradiance on the SCAs, especially in the LWIR bands. The cold shield surrounds the SCAs and is in good thermal contact with the cold focal plane. It extends out to the exit pupil of the telescope and defines the aperture of the system. The cold shield is surrounded by a low emissivity radiation shield which reduces the thermal load on the cryocooler by shielding the coldest parts of the focal plane assembly from the warm walls of the dewar.

The second function is to reduce the amount of stray light that reaches the focal plane. The cold shield includes internal baffles to impede stray light reflections from reaching the focal plane. The dimensions and spacing of the baffles as well as the highly absorbing surface finish are designed to minimize stray light.

3.2.6. Dewar Assembly

The dewar assembly puts together all the components listed above into a single unit, accurately holds the detector arrays in place at the focus of the optical system, and provides a vacuum enclosure so the focal plane assembly can be tested in the laboratory. The telescope interface ring is the precision interface between the telescope and the FPA, enabling final alignment of the FPA to the telescope and providing secure attachment points. The dewar assembly includes a barium fluoride window which is transparent to the entire range of wavelengths for this sensor. The window allows for convenient laboratory testing of the FPA and will reduce the possibility of contaminating the cold focal plane during on-orbit operation.

4. FPA PERFORMANCE

4.1. Detectors

The starting point for determining focal plane radiometric performance is the detectors. A common figure of merit for infrared detector performance is R_0A, the product of detector dynamic resistance at zero bias and the detector area. This quantity is a strong function of temperature. The minimum R_0A product at 75 K necessary to meet the focal plane performance requirements is 1×10^5 ohm-cm^2 for the InSb detectors and 95 ohm-cm^2 for the HgCdTe detectors. The noise contribution from the Si photodiodes at 75 K is negligible. The R_0A values achieved for MTI exceed the required levels, and the test data show that only band H is limited by detector noise. This was expected because the conversion gain of band H is very high.

4.2. Readouts

The readout integrated circuits also affect the sensitivity of the focal plane assembly. Very low noise is desired but must be balanced with the requirement for very large charge handling capacity for some of the spectral bands. The CTIA unit cell

circuit used for the MTI FPA provides very good noise performance by limiting the amplifier bandwidth and utilizing correlated double sampling. The limiting noise source for most bands is a combination of the read noise from the ROIC and the noise of the sensor electronics.

4.3. Filter Transmission

The optical filter transmission characteristics are tailored for each band. The two main considerations are in-band transmission and out-of-band rejection. Very good out-of-band rejection is required to perform precise spectral radiometry. In-band transmission must be high enough to meet the FPA sensitivity goals. Due to the optical system design, the angle of incidence to the filters varies across the focal plane. The spectral characteristics of interference filters depend on angle of incidence, so there are slightly different spectral characteristics at different focal plane locations within each band. These variations have been modeled and evaluated.

When the filter assemblies were fabricated, witness samples were made and measured for spectral transmission. Figures 6(a)-(d) show the measured transmission curves for each of the bands. Although some of the filters do not quite meet the predicted values for average in-band transmission, the overall focal plane sensitivity met requirements. In general, the filter spectral characteristics are quite good.

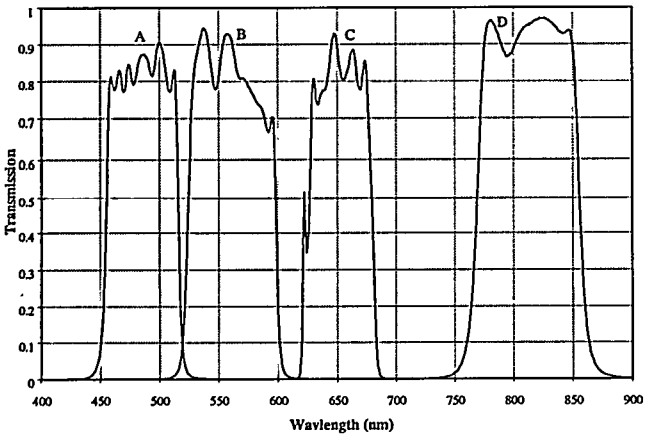

Figure 6(a). Filter transmission, bands A-D.

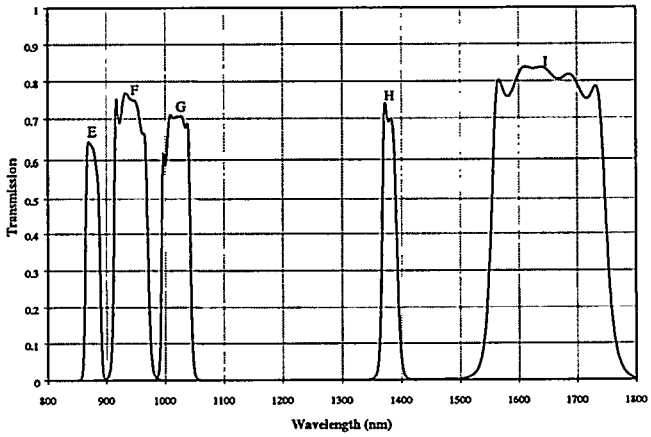

Figure 6(b). Filter transmission, bands E-I.

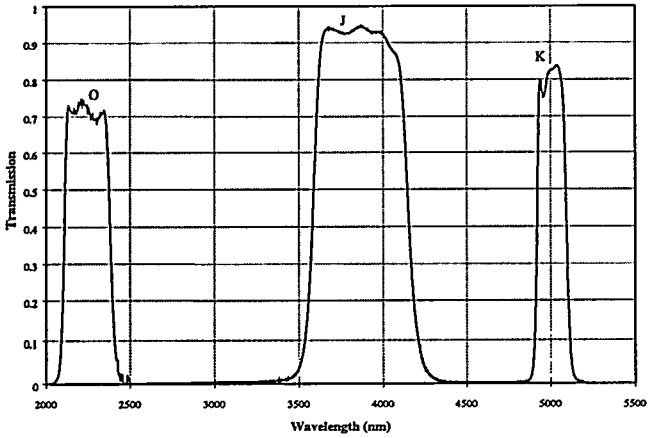

Figure 6(c). Filter transmission, bands O, J, and K.

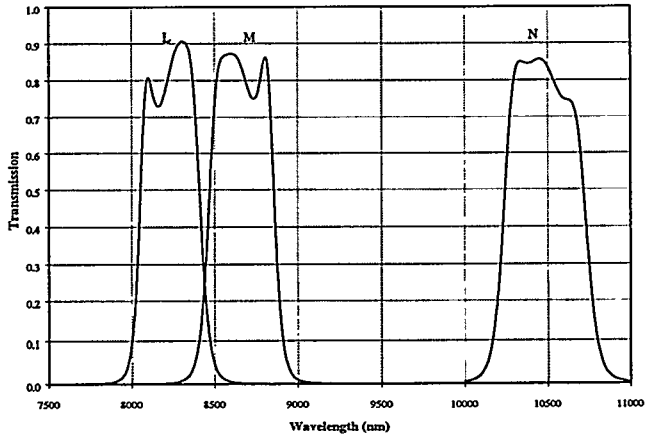

Figure 6(d). Filter transmission, bands L, M, and N.

4.4. Responsivity

The responsivity of the FPA is the voltage output divided by the photon irradiance and is expressed in V-cm^2-sec/photon. The responsivity is dependent on the optical filter transmission, the detector quantum efficiency, the feedback capacitance of the CTIA unit cell, and other gain factors of the ROIC. Before the flight SCAs were mounted to the pedestal of the focal plane assembly, radiometric measurements were performed on the SCAs without any of the spectral filters in place. The Si detectors were measured at 650 nm, the InSb detectors were measured at 3.6 - 4.1 μm, and the HgCdTe detectors were measured at 8 - 10.7 μm. The measured responsivity was adjusted for the MTI wavelength bands using the average in-band transmission values for the optical filters and the spectral response of the respective detector materials. The array average responsivity for each band is shown in Figures 7(a)-(b).

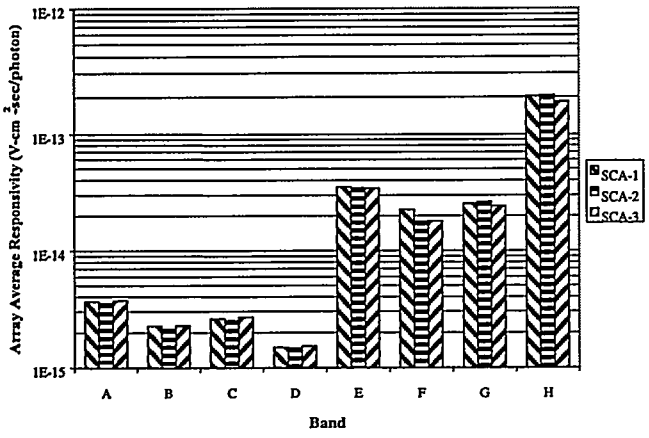

Figure 7(a). Average responsivity, bands A-H.

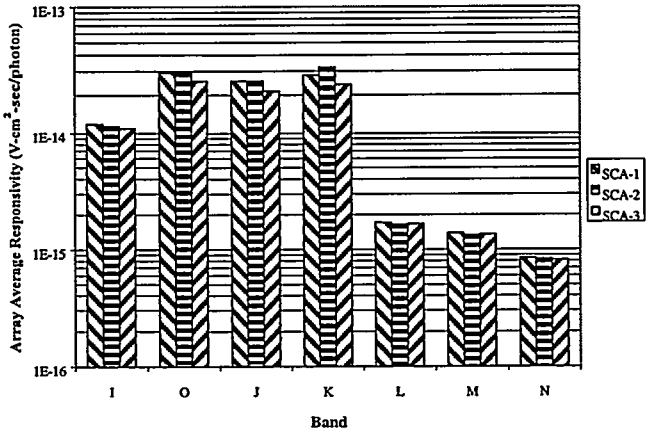

Figure 7(b). Average responsivity, bands I-N.

4.5. Noise Voltage

After the focal plane assembly was integrated with the rest of the payload, noise measurements were taken for all the spectral bands. These measurement were made with the retroreflector of the on-board calibration system in position, which presents a low photon background for all the spectral bands. This measurement includes the effects of detector R_0A, dark current shot noise, and the read noise of the ROIC. The noise measured, therefore, represents the actual noise floor that is expected in operation. The measured array average noise values are shown in Figures 8(a)-(b). The noise floor is fairly consistent for all the bands, except for band H, which indicates the limiting noise comes from the ROIC or the sensor electronics. Band H has very high conversion gain, so it was expected to be limited by detector noise. SCAs 1 and 3 of band L had higher noise also. The array averages for these bands were skewed by a number of noisy pixels. The pixel selection circuitry will allow most of these noisy pixels to be bypassed.

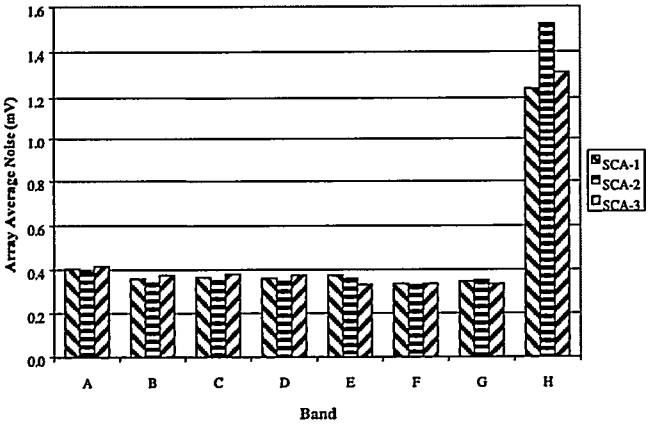

Figure 8(a). Average dark noise, bands A-H.

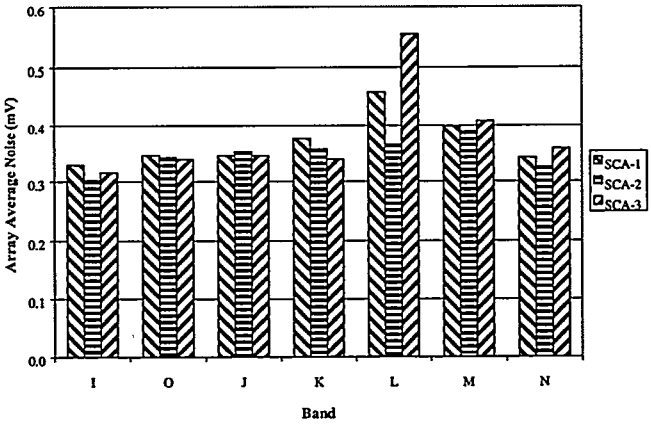

Figure 8(b). Average dark noise, bands I-N.

4.6. Noise Equivalent Irradiance

The noise equivalent irradiance (NEI) is the overall sensitivity parameter used to evaluate performance of the focal plane assembly. It represents the irradiance value which produces a signal value equal to the noise of the FPA and is calculated by dividing the responsivity by the noise. The lower the NEI, the better the performance. The NEI calculated for each spectral band is shown in Figures 14 and 15.

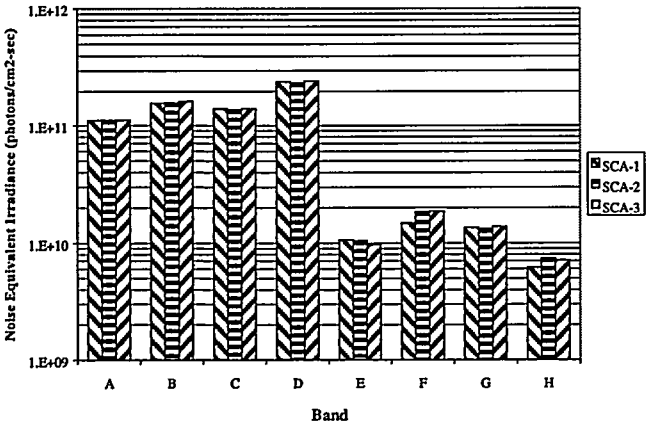

Figure 14. Average NEI, bands A-H.

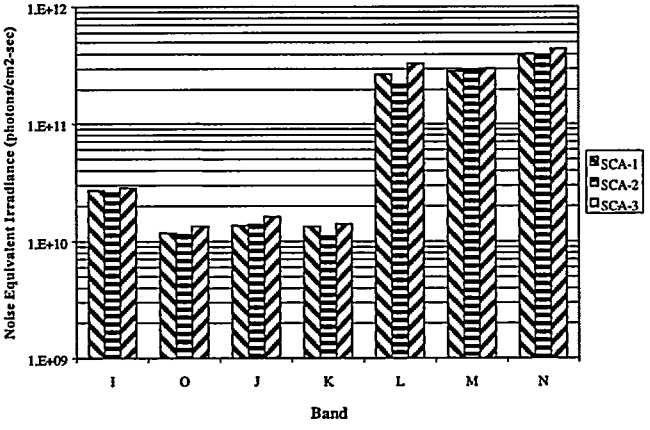

Figure 15. Average NEI, bands I-N.

4.7. Linearity

One important consideration for making accurate radiometric measurements is the linearity of response of the detectors and readout circuits. The voltage output of each pixel should be very nearly linear with incident irradiation. As it turns out, there is some nonlinearity over the range of irradiance expected. However, the response of each pixel is quite stable, and the deviation from linearity has been mapped out during payload calibration. The correction for nonlinearity will be part of the overall data analysis activity.

4.8. Thermal Load

A focal plane performance item of great concern is the thermal load that the focal plane assembly places on the cryocooler. Part of the thermal load is due to the electrical power dissipation in the detectors and readout integrated circuits. The largest part of the thermal load comes from radiative and conductive interactions of the focal plane assembly with the surrounding uncooled telescope structure. After integration of the FPA with the payload, the total cooling load on the cryocooler under nominal operating conditions was measured to be approximately 2.54 watts.

5. CONCLUSIONS

The MTI focal plane assembly embodies an approach to challenging technical requirements that combines proven detector and readout circuit technologies with innovative operational and packaging techniques. This overview of the focal plane assembly describes some of the key design features and performance measurements. The focal plane approach selected for MTI has produced a final product which meets all important design requirements and has potential for other multispectral imaging applications.

ACKNOWLEDGMENTS

Sandia is a multiprogram laboratory operated by Sandia Corporation, a Lockheed Martin Company, for the United States Department of Energy under contract DE-AC04-94AL85000.

This work was sponsored by the U.S. Department of Energy Office of Nonproliferation and National Security.

REFERENCES

1. C. B. Pease, *Satellite Imaging Instruments*, Chapter 14, Ellis Horwood Limited, Chichester, England: 1991.
2. C. B. Pease, *Satellite Imaging Instruments*, Chapter 12, Ellis Horwood Limited, Chichester, England: 1991.
3. C. B. Pease, *Satellite Imaging Instruments*, Chapter 16, Ellis Horwood Limited, Chichester, England: 1991.
4. P. G. Weber, B. C. Brock, A. J. Garrett, B. W. Smith, C. C. Borel, W. B. Coldius, S. C. Bender, R. R. Kay, and M. L. Decker, "Multispectral thermal imager (MTI) mission overview", *Proc. of SPIE*, this volume.
5. R. R. Kay, T. D. Henson, J. L. Rienstra, M. L. Decker, N. G. Rackley, P. J. Claassen, R. E. Kidner, R. B. Taplin, D. M. Bullington, K. D. Marbach, C. E. Lanes, B. C. Brock, P. G. Weber, S. C. Bender, B. W. Smith, W. B. Clodius, and C. C. Borel, "Multispectral thermal imager (MTI) payload overview", *Proc. of SPIE*, this volume.
6. T. D. Henson, L. Krumel, R. J. Blake, D. A. Byrd, W. Christensen, W. M. Rappoport, and G. Shen, "Multispectral thermal imager (MTI) optical assembly performance and integration of the flight focal plane assembly (FPA)", *Proc. of SPIE*, this volume.
7. M. R. Kruer, D. A. Scribner, and J. M. Killiany, "Infrared focal plane array technology development for Navy applications", *Optical Engineering* **26**, pp. 182-190, 1987.
8. J. T. Longo, D. T. Cheung, A. M. Andrews, C. C. Wang, and J. M. Tracy, "Infrared focal planes in intrinsic semiconductors", *IEEE Transactions on Electron Devices* **ED-25**, pp. 213-232, 1978.
9. J. L. Vampola, "Readout electronics for infrared sensors", Volume 3, Chapter 5, *The Infrared & Electro-Optical Systems Handbook*, Environmental Research Institute of Michigan, Ann Arbor, Michigan, 1993.